EFDA–JET–CP(14)01/20

M. Sertoli, J.C. Flanagan, M. Bacharis, O. Kardaun, A. Jarvinen, G.F. Matthews,
S. Brezinsek, D. Harting, A. Cackett, E. Hodille, I.H. Coffey, E. Lazzaro,
T. Pütterich and JET EFDA contributors

Impact of W Events and Dust on JET-ILW Operation

Impact of W Events and Dust on JET-ILW Operation

M. Sertoli[1], J.C. Flanagan[2], M. Bacharis[3], O. Kardaun[1], A. Jarvinen[4], G.F. Matthews[2], S. Brezinsek[5], D. Harting[2], A. Cackett[2], E. Hodille[2], I.H. Coffey[6], E. Lazzaro[7], T. Pütterich[1] and JET EFDA contributors*

JET-EFDA, Culham Science Centre, OX14 3DB, Abingdon, UK

[1]Max-Planck-Institut für Plasmaphysik, 85748 Garching, Germany
[2]EURATOM-CCFE Fusion Association, Culham Science Centre, OX14 3DB, Abingdon, OXON, UK
[3]Blackett Laboratory, Imperial College London, Prince Consort Road, London, UK
[4]Aalto University, Association Tekes, Espoo, Finland
[5]Forschungszentrum Jülich GmbH, EURATOM Association, 52425 Juelich, Germany
[5]Queen's University, Belfast, BT7 1NN, UK
[6]Istituto di Fisica del Plasma C.N.R., Milan, Italy
** See annex of F. Romanelli et al, "Overview of JET Results", (24th IAEA Fusion Energy Conference, San Diego, USA (2012)).*

Preprint of Paper to be submitted for publication in Proceedings of the
21st International Conference on Plasma Surface Interactions, Kanazawa, Japan
26th May 2014 - 30th May 2014

ABSTRACT

The occurrence of transient impurity events (TIE) leading to intense radiation spikes in JET plasma discharges has been studied since the installation of the ITER-like Wall (ILW). To generate the observed average increase in radiated power of 1.5MW, a 100μm-radius sphere of solid W dust would be required. The drop in plasma energy caused by W-TIEs is fully recovered in 90% of all cases, only 1% inducing a longer term loss in plasma energy which sometimes leads to the shut-down of plasma operation. TIEs are correlated with disruptions and with measurements of the dust mobilized by disruptions using the high resolution Thomson scattering (HRTS) diagnostic. The dust characteristics giving rise to TIEs have been studied using the dust transport code DTOKS and the 1D impurity transport code STRAHL

1. INTRODUCTION

The understanding of dust production, control and its effects on plasma operation is a major concern not only for future tokamaks such as ITER, but also for present-day devices such as JET. Transient impurity events (TIEs, also called UFOs), visible as sharp increases in the total radiated power (Figure 1b) similar to what caused by laser ablation experiments, have the potential to terminate the discharge due to extreme radiation losses in JET.

This contribution reports on the study of TIEs observed in JET since the installation of the ITER-like wall (ILW), on their impact on regular plasma operation and their relation to dust. The responsible impurities have been studied using vacuum ultra–violet (VUV) spectroscopy. Their occurrence has been correlated with plasma geometry, arcs from lower-hybrid (LH) antennas, reciprocating probe (RCP) plunges and laser blow-off (LBO) (section 2). Correlation analysis with plasma parameters has been performed (section 3) and comparison with independent estimates on the dust mobilized by the disruptions obtained using the high resolution Thomson scattering (HRTS) diagnostic and correlation with disruption occurrence is reported (section 4). The limited amount of TIE-induced disruptions are not reported since they have been intensively analysed elsewhere (see e.g. [1]). Modelling of the particle ablation has been performed using the dust code DTOKS. The 1D impurity transport code STRAHL has been employed to estimate the parameters of the dust particles which could lead to the observed increases in radiated power (section 5). A discussion and conclusions are given in section 6.

2. TIE IDENTIFICATION AND GEOMETRICAL DEPENDENCIES

The occurrence of TIEs has been analysed in all JET discharges in range JET Pulse No's 80128 –85699 with plasma current $I_p > 1$ (MA). A total of 3388 events have been detected in 4144 discharges (~23h of plasma), for an average of 1 event every 25 seconds of plasma. For each event, a database has been built with the responsible impurities, the maximum excursion in total radiated power and drop in plasma energy due to the event. The plasma current, plasma energy, ohmic and externally applied heating powers, radiated power, line averaged electron density, geometrical parameters

(distance form inner and outer limiter, strike-point configuration, elongation, triangularity, volume), the vacuum toroidal magnetic field, q_{95} as well as confinement factors (H89 and H98(y.2)) and the Greenwald fraction have also been tabulated for correlation purposes.

A second database using the same selection criteria containing the total plasma operation time (in steps of 10ms) for each correlation quantity provides the normalization parameters for the event distributions. A TIE rate (# of events/operation time = Hz) can therefore be evaluated, its error bar given by the propagation of the statistical error of the number of events, equal to its square root.

2.1. RESPONSIBLE IMPURITIES

The VUV-spectrometers used for this study can distinguish Ni; Fe;Cr;Cu; Al and W spectral features [2] and the events have been divided in three element groups:

i) **W** (51% of all events): events where W is detected (usually alone).

ii) **Ni/Fe/Cr** (26%): events where either Ni, Fe or Cr are visible (usually in paris or triples, from either Inconel structural material or steel support structures).

iii) **Others** (27%): events where either Al or Cu are observed (< 1%) or no responsible impurity can be identified.

An example of the time evolution of the line intensities of W, Ni and Fe is given in figure 1 for two undefined and one (the last one) W event.

For about 10% of the W events either Ni, Fe or Cr have also been detected. Since the ILW includes PFCs of different material mixtures (bulk W, W-coated CFC, Becoated Inconel, bulk Be [3]) and the dust particles involved may contain a combination of them, these element groups should be interpreted more as a detection limit of the spectrometers than as a strict distinction between particle composition. Nevertheless, the rationale behind the element groups is confirmed by those events whose cause could be identified. Events induced by LH-arcs (5 events out of 19 detected) and RCPs (22 events out of 217 plunges) are dominated by Ni/Fe/Cr, consistent with the material of the LH launcher (stainless steel) and of the probe shaft (Inconel / steel). The TIEs correlated with LBO injections (41 events out of 55 LBOs) show an element distribution consistent with the injected materials: 38% Ni, 18% W and 44% Mo or Zr, the latter two included in the Others group defined above since not detected by the VUV spectrometers used. The analysis presented from now on excludes the events listed above and concentrates on the 3320 events whose direct cause could not been determined.

2.2. GEOMETRICAL DEPENDENCIES

The probability of TIEs occurring in limited plasmas is very low, only 8% of all the detected events taking place over the ~7h of limited-plasma operation (table 1). Most events occur in diverted configurations, exhibiting a 57mHz rate if the outer strikepoint is on a horizontal tile while drops to < 1mHz If the outer strike-point is on a vertical tile. This difference can be interpreted noting that the horizontal part of the divertor is a deposition zone for material coming from the main chamber. Dust

accumulating here may then be mobilized by transient heat and particle loads (e.g. ELMs) or thermal stresses leading to the observed TIEs.

3. IMPACT ON PLASMA OPERATION AND PARAMETRIC DEPENDENCIES

Throughout the ILW campaigns, a limited number of TIEs lead to pulse termination due to extreme radiation losses leading to a collapse of the temperature proles (e.g. the W event in JET Pulse No: 81765 at 3 10.5s). To investigate the effect of such each event on the background plasma, the loss in plasma energy (e.g. in Figure 1a) and its recovery after 200ms has been tabulated. The results are shown in Figure 2 and summarized in table 2, giving the conditional probability of an event of a specific element group leading to a long term percentage loss in plasma energy WP with respect to the value before the event occurred W_P.

The plasma recovers completely in 94% of all cases. W particles are clearly the most dangerous, 6% of these leading to moderate losses and, in 1% of all cases to extreme losses > 60%. The latter account for a total of 25 events. If each of these were to lead to the termination of the plasma, this would translate in a 0.6% TIE-induced plasma termination rate. This is a factor 5 lower than the unintentional disruption rate observed in the last years of JET-C (3.4%) and an order of magnitude lower than what observed in the 2011-2012 JET-ILW campaigns (10%) [1].

3.1. PARAMETRIC DEPENDENCIES

The parameter space within which TIEs occur is broadly populated and no clear scenario of highest TIE-rate has yet been found. Nonetheless, univariate distributions show that the rate increases with gas puff rate Φ_D, upper triangularity δ_u, closeness of the plasma to the inner wall and heating power normalized to the L-H power threshold P_{heat} / P_{thr} [4]. These trends are confirmed by multivariate regression analysis which has been performed on a sub-set of the original database with stricter selection rules: lower-single null (LSN) discharges; $I_P > 1$MA; at-top only ($\delta I_P / I_P < 1\%$); stationarity ($\delta P_{ext} / P_{ext}$ and $\delta \langle n_e \rangle / \langle n_e \rangle < 5\%$, $-0.05 < \langle (dW_{DIA} / dt) = W_{DIA} \rangle < 0.35$). All quantities have been interpolated on a time axis with 50ms time resolution and averaged over 500ms. Here, I_P the plasma current, P_{ext} the external heating power, $\langle n_e \rangle$ the line averaged electron density, W_{DIA} the diamagnetic energy.

The results (equation 1), based on a condensed table averaging all quantities per discharge, show the same qualitative and quantitative dependencies as the univariate distributions

$$\frac{P}{1-P} = 3 \cdot 10^{-4} \times \cdot (\delta_u + 1)^{3.5 \pm 2.4} \cdot (R_{in} - R_{wall})^{-1.1 \pm 0.6} \cdot \Phi_D^{0.33 \pm 0.12} \cdot (P_{heat} / P_{thr})^{0.43 \pm 0.24} \qquad (1)$$

where $R_{in} - R_{wall}$ is the distance of the plasma from the inner wall at $z = 0$. The errors indicate twice the estimated standard deviation. Multiplying the exponents by 5σ of the regression variables one obtains an indication of the range within which the plasma parameters can influence the probability provided the model with the selected variables is to a reasonable approximation correct: 0.97;

–1:65; 2.0; 1.44, for triangularity, distance from the inner wall, gas puff and normalized heating power respectively.

4. CORRELATION WITH DISRUPTIONS

If disruptions and TIEs were cause-effect related, one would expect TIEs to occur more often either in discharges following a disruption or in discharges approaching a disruption. Within 4 discharges after a disruption the rate is 50% higher than the 40mHz average while for events occurring further away, the value is instead 25% lower. In order to account for possible cumulative effects due to disruptions occurring in subsequent discharges or few discharges from one another, the events have been re-binned limiting the distance of the event from the 2nd – last disruption. Whether the selection is performed on the last disruption only or setting a limit of the 2nd – last disruption to > 10 plasma discharges, > 20 or > 30 discharges, the decreasing trend is still observed.

No relation of such kind has instead been found when correlating the TIE-rate to the number of discharges approaching a disruption. It can therefore be clearly stated that TIEs do not have a direct effect on disruptions, but that disruptions have an effect on the TIE rate. This could be due either to a redistribution of particles onto more accessible areas of the machine or through a generation of particles.

4.1. COMPARISON WITH HRTS DUST DATA

The time evolution of the TIE rate has been correlated with estimates of the dust mobilized by disruptions determined by particle scattering (Rayleigh, Mie etc.) recorded with the HRTS diagnostic system [5, 6]. The HRTS detects only particles passing the laser beam (1064nm, 5J, 20ns pulses, 20Hz) during the 1–2s after the current quench, so only a small fraction of the particles present in the machine is covered. Since TIEs are detected during the plasma discharge, in order to compare these two datasets only the events occurring within 5 discharges after the last disruption have been considered. The bins have been kept rather large (300 plasma discharges) to ensure a relevant number of disruptions in each bin. The temporal evolution of the TIE-rate (black bars in Figure 3) is qualitatively well reproduced by the rate of HRTS dust events normalized to the number of disruptions (green). The first two points of the HRTS data have been left out of range in order to better compare the remaining part of the range. A few possible HRTS outliers (percentage error exceeding 50%) have been highlighted with red circles. The ne structures in the time evolution of the TIE rate are well replicated by the HRTS analysis and the large drop in rate occurring in the first 4 1200 discharges is seen by both analysis by a similar factor (TIEs falling of a factor 2:5, HRTS of a factor 3:3).

5. MODELLING OF TIES

Modelling of dust trajectory and ablation has been undertaken using the code DTOKS [7]. The physical model includes charging and heating of the dust particle, and the equation of motion

accounts for the Lorentz force, ion drag and gravity. The particles are assumed of spherical shape and the composition, size, initial velocity and injection angles are input parameters which have been scanned in range: [10; 100]μm, = [1, 25] m/s and = [–90, +90 deg]. The background plasma has been taken from an EDGE2D Eirene simulation of JET Pulse No: 82550 in time range [15, 16] s. Only the size and angle scan of a W particle injected from the outer strike-point position with velocity 10m/s will be discussed here.

Figure 4 displays the poloidal cross-section of the plasma, showing the position of ablation of a W particle along its flight path. The different colours correspond to particles sizes 100 blue, 75 lilac, 50 red, 25 green and 10μm orange. The larger the particle mass the deeper inside the plasma core it will ablate, but the ratio between the total injected mass and the mass ablated in the plasma core (screening factor) reaches a plateau value of 5 50% for particle sizes above 20 (μm).

For the particles reaching the plasma core, the 1D impurity transport code STRAHL [8] has been used to simulate the observed increase in total radiated power caused by TIEs. The perpendicular transport in the SOL and core plasma is simulated using a diffusive and convective ansatz. The diffusion has been set to typical values observed in fusion devices: 0.5 (m^2/s) in the SOL, 3 at the pedestal top, decaying to 0.5 in the plasma centre. The convection velocity was chosen such that $-v/D = \nabla n_e / n_e$. Recycling at the wall has been switched off, imposing that the particles do not re-enter the plasma the moment they reach the wall. The main plasma parameters, have been taken from the EDGE2D-Eirene simulations used for the DTOKS runs and using the results from DTOKS, the source position has been set to 1.5cm inside the separatrix.

he number of ablated ions needed to generate the observed increase in radiated power is of the order of $2 \cdot 10^{17}$ which, accounting for a 50% screening of the dust particle evaluated through DTOKS, leads to an initial particle size of ~115μm. Since not all TIEs have occurred with the plasma parameters of JET Pulse No: 82550, using the temperature and density proles from HRTS and assuming local-ionization-equilibrium, the particle size reduces to 103μm. Accounting for the total number of detected W-events (1697), 0.42g of W dust is needed to generate them. The average size of such particles is of the order of the droplets released during the bulk-W melt experiments [9].

6. DISCUSSION AND CONCLUSIONS

The occurrence of transient impurity events has been studied in JET-ILW analysing their impact on plasma operation and correlating their rate with plasma parameters, disruptions and independent estimates on dust mobilized by disruptions using the HRTS diagnostic.

The excellent correlation between the time evolution of the TIE rate and the dust events detected by the HRTS diagnostic conrms the assumption that TIEs are caused by dust particles. A general decreasing trend of both quantities suggests that the amount of dust in JET-ILW is decreasing with time and the rate of particle-creation appears to be lower than that of its destruction. Disruptions are found to have an enhancing effect on the TIE rate which increases by a factor 1.5 with respect to the

average value in discharges following a disruption. It is still not clear if this is because disruptions create particles or merely redistribute them onto more accessible parts of the torus. Less than 1% of all TIEs have caused a long term loss in plasma energy which have sometimes led to discharge termination. This translates in a rate of TIE-induced plasma termination risk of 0:6%, much lower than the unintentional disruption rate in both JET-C and JET-ILW. The size of the particles responsible is ~100μm, of the same order as what estimated from the W melt experiments [9]. The W-coated CFC tiles probably the origin of the W dust since delaminations have been observed on several tiles [10]. For future machines such as ITER it is important to understand this so to optimize the design of the plasma facing components.

Future studies should include the effects of ELMs since they could lead to the initial mobilization of the dust. Experimental eort should be dedicated to constrain modelling parameters so to better understand the physical processes at play. A benchmarking between two dierent dust-transport codes (DTOKS [7] and DUSTTRACK [11]) has already started.

ACKNOWLEDGMENTS

This work was supported by EURATOM and carried out within the framework of the European Fusion Development Agreement. The views and opinions expressed herein do not necessarily reflect those of the European Commission.

REFERENCES

[1]. de Vries P.C. et al; 2014 Physics of Plasmas (1994-present) **21**
[2]. Sertoli M. et al; 2014 Physica Scripta **2014** 014014
[3]. Matthews G. 2013 Journal of Nuclear Materials **438**, Supplement S2–S10
[4]. Snipes J.A. et al; 2000 Plasma Physics and Controlled Fusion **42** A299
[5]. Pasqualotto R. et al; 2004 Review of Scientic Instruments **75** 3891–3893
[6]. Giovannozzi E. et al; 2010 Review of Scientic Instruments **81** 10E131
[7]. Bacharis M. et al; 2010 Physics of Plasmas (1994-present) **17**
[8]. Dux R. STRAHL User Manual Laborbericht 10/30, IPP Garching, September 2006
[9]. Coenen J. I8, this conference
[10]. Widdowson A. et al; 2014 Physica Scripta **2014** 014010
[11]. Lazzaro E. et al; 2012 Plasma Physics and Controlled Fusion **54** 124043

	Total plasma time	Number of events	Event rate	Most abundant element
	(h)		(mHz)	(% in that configuration)
Limiter	6.8	260	10	Ni/Fe/Cr (50 %)
Horiz. Outer SP	14.6	3047	57	W (55 %)
Vert. Outer SP	1.7	4	< 1	-

Table 1: Total plasma time (h), number of events, event frequency (mHz) and most probable element for limited (Limiter) and diverted configurations with the outer strike-point on a horizontal target plate (Horiz. Outer SP) or on a vertical one (Vert. Outer SP).

	Full recovery $\delta W/W < 5\%$	Moderate loss $10 < \delta W/W < 30\%$	Extreme loss $\delta W/W > 60\%$
	(% of events)	(% of events)	(% of events)
W	91	6	1
Ni/Fe/Cr	97	2	< 1
Others	97	2	< 1
total	94	6	< 1

Table 2: Long-term (> 200ms) percentage loss in plasma energy for the different element groups.

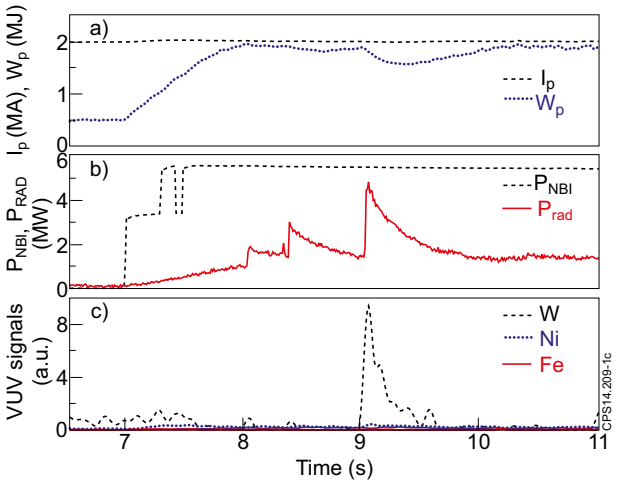

Figure 1: Example of TIEs occurring in JET Pulse No: 81611: (a) plasma current and plasma energy; (b) NBI and radiated power; (c) VUV signals for W, Ni and Fe. Colour coding as in label.

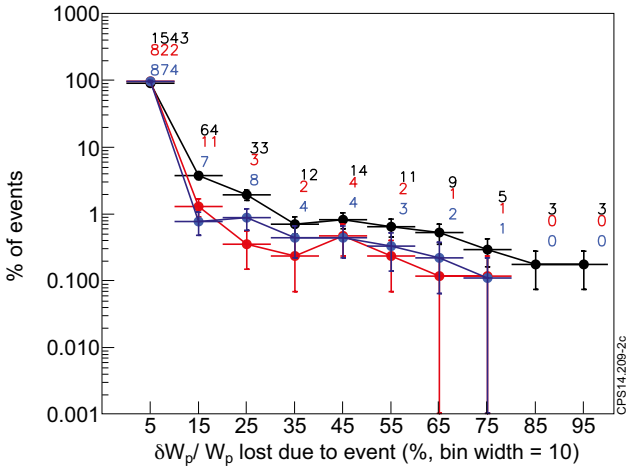

Figure 2: Conditional probability of an event leading to certain percentage loss in plasma energy 200 ms after the event (0% = full recovery, 100% = complete loss). W in black, Ni/Fe/Cr in red, Others in blue, the numbers indicating the # of events in each bin for each element group (same colour coding).

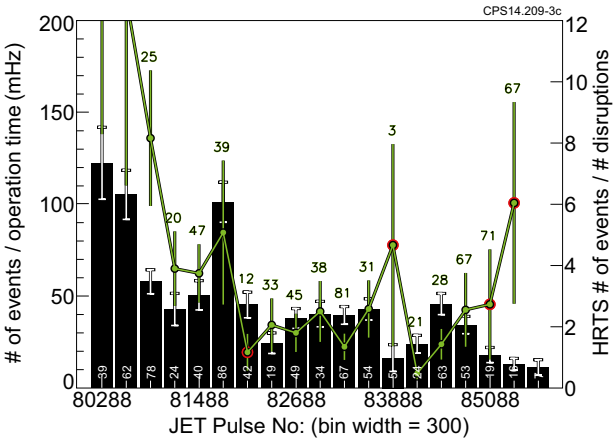

Figure 3: TIE-rate evolution in time (black bars) and HRTS number of dust events (green) versus discharge number. The white and green numbers on the graph give the number of TIEs and the number of disruptions in each bin respectively. Red circles highlight possible outliers in the HRTS data.

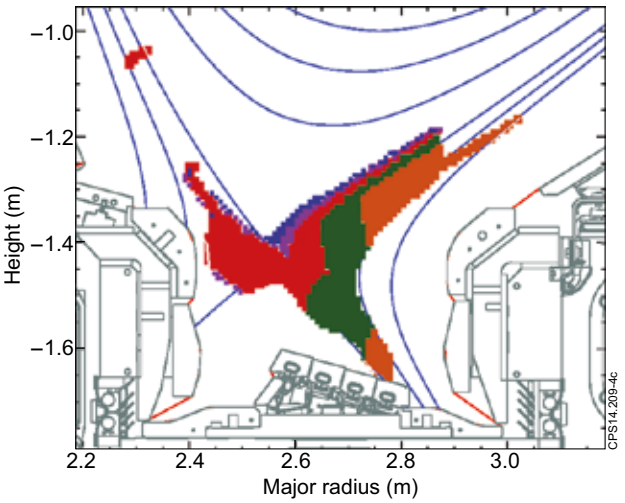

Figure 4: Poloidal cross-section of plasma discharge JET Pulse No: 82550 at 15.5 seconds. Coloured regions in the divertor indicate the average ablation position for DTOK results with the parameters described in the text.